Monte Carlo Simulation of Singlet Energy Migration and Trapping in Nonrandom Chromophore Distributions Generated by Photoreaction in Glassy Polymer Matrices

Zhiyu Wang, David A. Holden,† and Frederick R. W. McCourt*

Guelph-Waterloo Centre for Graduate Work in Chemistry, Department of Chemistry, University of Waterloo, Waterloo, Ontario, Canada N2L 3G1

Received May 8, 1990; Revised Manuscript Received August 2, 1990

ABSTRACT: A Monte Carlo simulation was conducted of singlet energy migration and trapping in the particular type of chromophore distribution generated when a reactant is converted photochemically under diffusion-free conditions into a product that acts as a long-range quencher. The simulation proceeded in three stages: generation of randomly distributed donors, conversion to nonrandom distributions of donors and quenchers by modeling of the photoreaction, and simulation of singlet electronic energy migration and trapping by the Förster mechanism on distributions obtained at different degrees of conversion. The sensitivity of the model to such parameters as ensemble size and number of donors and quenchers considered around each excited-state chromophore was investigated. In the nonrandom distributions generated in this simulation quencher chromophores tended to be spaced a minimum distance R_{DQ} apart, where R_{DQ} is the Förster radius for donor-quencher transfer. Conversion-time curves were generated that show the same leveling off with time as the experimental data. Donor decay profile functions $G(t)$ were shown to differ significantly for nonrandom and random distributions at the same bulk chromophore concentrations. The simulated energy-transfer functions were used to construct donor fluorescence decay curves, which were then compared in detail with fluorescence decays obtained in earlier work for 2-naphthyl acetate irradiated in glassy poly(methyl methacrylate) matrices. Experimental and simulated decay curves were found to correspond within the limits of experimental accuracy.

Introduction

The problem of electronic excitation transport and trapping in chromophoric systems has been the subject of numerous theoretical treatments in the literature,[1-13] as well as modeling by Monte Carlo simulation.[14-22] Recently, there have been efforts to extend such treatments to anisotropic, spatially nonrandom, or even highly organized, chromophore ensembles.[17,18,23-29] Such extensions are relevant to energy migration and trapping in such important physical systems as polymers, membranes, and liquid crystals, for which considerable experimental data have been gathered.

Recently, we obtained experimental results establishing that an important general class of photoreaction, namely the conversion of a reactant under diffusion-free conditions to a photoproduct capable of acting as a long-range quencher, gave unusual energy-transfer behavior.[30] On the basis of the effects of annealing or softening of the glassy polymer matrix by solvent treatment on the donor fluorescence decays, it was concluded that long-range quenching by the photoproducts suppressed the formation of quenchers closer to each other than R_{DQ}, the Förster radius for donor-quencher energy transfer. The result was a spatially nonrandom ensemble of donors and traps whose fluorescence decay was clearly different from that predicted by models based on randomly distributed chromophores.[2,13] These results were significant because an appreciable fraction of the photochemical reactions responsible for polymer photodegradation may result in spatially nonrandom chromophore distributions.

We were interested in exploring the properties of nonrandom chromophore distributions created by a photochemical reaction. Since energy migration and transfer in nonrandom chromophore ensembles are difficult to represent analytically, we approached the problem by employing Monte Carlo simulation. The present publication describes a Monte Carlo study of the generation of nonrandom chromophore distributions as a result of a gradual photoreaction in an amorphous matrix, as well as a Monte Carlo simulation of singlet energy transport and trapping in these spatially nonrandom distributions. In addition to exploring the properties of the nonrandom distributions and the sensitivity of the simulation to various model parameters, we describe the results of a detailed comparison of the simulation behavior with our earlier experimental results,[30] which dealt with the photochemical Fries reaction of 2-naphthyl acetate[31-33] in poly(methyl methacrylate) (PMMA), shown in eq 1.

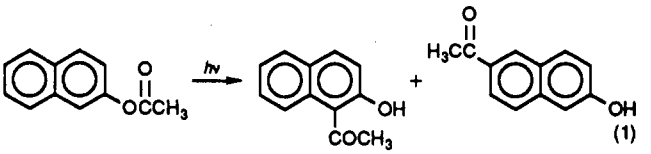

(1)

Description of the Algorithm

The numerical simulation consisted of three linked parts, each of which requires a separate Monte Carlo calculation. The components were (1) generation of a random distribution of donor chromophores, understood to be trapped in a homogeneous glassy matrix, (2) conversion of a certain fraction of the donor chromophores to photoproduct quenchers by simulation of a stepwise photoreaction occurring under diffusion-free conditions, and (3) Monte Carlo simulation of electronic energy transport and trapping within the chromophore distributions produced in step 2.

Generation of Initial Distributions. In the first step of the simulation a random distribution of N_0 donor chromophores was created within a cubic box of volume V. Since the continuous phase in our experimental study was glassy poly(methyl methacrylate), the positions of the donor chromophores in the simulation remained fixed on selection. In a typical computation the box had a side

† Deceased.

0024-9297/91/2224-0893$02.50/0

length of $10R_{DQ}$, where R_{DQ} is the Förster radius for dipole–dipole excitation transfer between a donor D and a photoproduct quencher Q, so that $V = 10^3 R_{DQ}^3$. Typical values of N_0 were 500, 1000, or 2000, which for $R_{DQ} = 2.5$ nm, as in our experimental system, correspond to initial concentrations of donors of from 0.05 to 0.2 M.

In order to maintain as close a resemblance to a real physical system as possible, the effect of restricting the distance of closest approach of any two donor chromophores to a value of R_0 was examined. In a typical run R_0 was set equal to $0.2R_{DQ}$, corresponding to a closest approach of 0.5 nm. It was observed that energy transport and trapping at these chromophore concentrations was insensitive to the choice of R_0 between $0.1R_{DQ}$ and $0.3R_{DQ}$. The x, y, and z coordinates of each chromophore were selected by independent calls to the pseudorandom number generator. Following generation of all N_0 coordinate sets, those chromophores lying closer together than R_0 were rejected and new coordinates were generated for replacement chromophores. The procedure was repeated until a satisfactory configuration was attained.

Generation of Spatially Nonrandom Donor/Quencher Ensembles. Following electronic excitation of a donor chromophore there are four possible competing processes: (1) deactivation to the ground state by fluorescence or nonradiative decay; (2) photochemical reaction to generate a quencher; (3) excitation hopping to another donor; or (4) excitation trapping by an existing quencher. To minimize computation time the relative probabilities of processes 2, 3, and 4 were computed, and process 1 was accounted for by multiplying the resultant donor decay profile functions by $\exp(-t/\tau_f)$, where τ_f is the donor fluorescence relaxation time in the absence of quenchers. Previous work on the photo-Fries reactions of naphthyl esters established quantum yields of starting material disappearance of 0.05–0.10.[32] The photo-Fries reaction has also been found to be insensitive to solvent viscosity.[31] Accordingly, a quantum yield of 0.10 was chosen for the simulation, so that the rate constant for process 2 becomes

$$k_2 = 0.1/\tau_f \tag{2}$$

The rate constant for transfer to a particular donor by the Förster mechanism is

$$k_3 = \frac{1}{\tau_f}\left(\frac{R_{DD}}{R_{il}}\right)^6 \equiv w_{il} \tag{3}$$

where R_{DD} is the Förster radius for transfer between donor chromophores, and R_{il} is the separation between chromophores i and l.[2] Förster energy transfer is treated in its spherically averaged form, in conformity with other studies in the literature.[9,13,20] The rate expression for Förster transfer to a quencher j a distance R_{ij} away is

$$k_4 = \frac{1}{\tau_f}\left(\frac{R_{DQ}}{R_{ij}}\right)^6 \equiv v_{ij} \tag{4}$$

Again, the orientation dependence of the transfer rate is not considered. The relative probabilities of the three processes for a particular donor chromophore i are then given by eqs 5–7

$$p_{i2} = 0.1/\tau_f k \tag{5}$$

$$p_{i3l} = w_{il}/k \qquad l = 1, 2, ..., N_D \quad (l \neq i) \tag{6}$$

$$p_{i4} = \sum_{j=N_D+1}^{N_D+N_Q} v_{ij}/k \tag{7}$$

where

$$k = \sum_{l=1}^{N_D} w_{il} + \sum_{j=N_D+1}^{N_D+N_Q} v_{ij} + \frac{0.10}{\tau_f} \tag{8}$$

is the sum of the rate constants for all processes that lead to removal of the excitation from donor i, and N_Q is the number of quenchers generated. In eq 6 it is necessary to know the destination of the excitation explicitly, and therefore all donor–donor transfer probabilities must be evaluated separately. This is not the case for transfer to a quencher, and therefore a lumped transfer probability is calculated in eq 7.

Insteady of randomly redesignating a certain number of donors as quenchers, our Monte Carlo simulation generates each new quencher subject to the relative magnitudes of the probabilities in eqs 5–7. Following random selection of a donor chromophore i the relative probabilities characteristic of the surrounding configuration are computed and ranked in accumulative order:

$$(p_{i2}, p_{i2}+p_{i3l}, ..., p_{i2}+...+p_{i3N_D}, p_{i2}+...+p_{i3N_D} + p_{i4} = 1) \tag{9}$$

A pseudorandom number between 0 and 1 is used to select an event by comparison with the elements of eq 9. This procedure is continued until the degree of conversion reaches a target value y:

$$y = N_Q/(N_D + N_Q) = N_Q/N_0 \tag{10}$$

In the interest of minimizing the time spent evaluating the probabilities in eqs 6 and 7, we investigated how many nearest-neighbor donors and quenchers about the photoexcited donor actually had to be considered for energy transfer and trapping before limiting behavior was attained. At the low donor and quencher concentrations employed in our simulation, we found that limiting aggregate transfer probabilities were attained after consideration of only a few nearest donors and acceptors. Consequently, most of the generation of spatially nonrandom distributions, as well as modeling of excitation energy transfer and trapping on these distributions, were conducted with calculation of eq 6 for the five nearest-neighbor donors, and eq 7 for the three nearest-neighbor quenchers.

Most authors have used reduced donor and quencher concentrations, defined in terms of the Förster radii as shown in eqs 11 and 12 in theoretical models of energy migration and trapping.[9,13,17,20]

$$C_D = \frac{4\pi R_{DD}^3}{3}\left(\frac{N_D}{V}\right) \tag{11}$$

$$C_Q = \frac{4\pi R_{DQ}^3}{3}\left(\frac{N_Q}{V}\right) \tag{12}$$

For ease of comparison with the work of others, the donor and quencher concentrations in the present study are expressed in reduced units. Typical initial values of C_D in our simulations ranged from 0.27 to 0.52. These values were low and probably explain why the summation of probabilities in eq 6 could be truncated after consideration of so few terms.

Simulation of Energy Transport and Trapping. Excitation hopping and transfer to quenchers was modeled for the particular nonrandom chromophore distributions generated in step 2 by using a modification of the procedure of Engström et al.[20] These authors used the concept of periodic boundary conditions to allow simulations to

proceed when a chromophore close to one face of the cube was excited. We were reluctant to introduce periodic boundary conditions into our system, because the translation of the chromophore distributions into adjacent cubes risked placing quenchers along the common face less than a distance R_{DQ} apart. Since we regarded this spearation of quenchers by distances on the order of R_{DQ} to be the central feature of the nonrandom distribution, we have eliminated the problem of edge effects in a different way. The initial excitation of donor chromophores was confined within a central cube of side length $2R_{DQ}$ within the larger cube of side length $10R_{DQ}$. At the low donor concentrations in our simulation, the excitation seldom wandered near the edge of the larger cube, and yet the chromophore distributions within the central box were entirely representative of those in the larger configuration.

For better comparison with experiment we eliminated the photo-Fries reaction (eq 5) from the energy migration and transfer simulation. This was done because the experiments (which the simulation was intended to model) were conducted with low-intensity pulsed excitation and single-photon-counting detection on very much larger chromophore ensembles, so that the extent of additional conversion to photo-Fries products during measurement of the donor fluorescence decays was negligible. A further justification for eliminating eq 5 is that for most of the simulations, the dominant deactivation process was Förster transfer to a quencher, so that the magnitude of p_{i2} in eq 5 was very small.

The simulation calculates the survival probability $G(t)$ of the excitation within the ensemble of donor chromophores, given that it can undergo both transfer and trapping within the surrounding configuration. The relative rates of the two processes are given by eqs 6 and 7. Transfer to a quencher is assumed to be irreversible, so that an individual simulation ends once this process occurs. The simulation keeps track of the location of the excitation, recomputing the index of probabilities after every transfer to another donor. The residence time in a given state i is represented by

$$\Delta t_i = -(\ln a_i)/k \tag{13}$$

where a_i is a pseudorandom number between 0 and 1, and k is now given by eq 14.

$$k = \sum_{l=1}^{N_D} w_{il} + \sum_{j=N_D+1}^{N_D+N_Q} v_{ij} \tag{14}$$

Each simulation was allowed to proceed either until deactivation of the excitation occurred or until a maximum run time had been exceeded.

Computational Details. Programs were written in FORTRAN. A typical simulation involved the generation of 200–400 nonrandom configurations, each containing a total of 1000 chromophores, and each configuration was used for 50 simulations of excitation energy migration and trapping. Each run, corresponding to a particular degree of conversion of donors to quenchers, required 10–12 CPU hours on a VAX 11/785, or about 2 CPU hours on a Silicon Graphics 4D/240.

Modification of Simulation Data for Comparison with Experiment. The experimental data that we were most interested in comparing with the Monte Carlo simulation consisted of donor fluorescence decays measured for different degrees of conversion to photoproducts. Accordingly, the ensemble of survival probabilities $G_i(t)$ generated by the energy-transfer simulation was sorted into data channels, each 0.2230 ns wide. The simulated donor fluorescence decay curves were then given by

$$I_D(t) = G(t) \exp(-t/\tau_f) \tag{15}$$

where $G(t)$ represents the donor decay profile function. The donor fluorescence lifetime τ_f, measured in the absence of photoproducts, was 23.236 ns.[30] These simulated decay curves were reconvoluted with a real instrument response function $P(t)$:

$$I_F(t) = \int_0^t P(t')I_D(t-t')\,dt' \tag{16}$$

The resulting decays were then plotted on the same scale as the experimental decay curves, and the two types of curves were compared by using standard statistical tests for quality of fit: reduced χ^2, analysis of weighted residuals, and inspection of the autocorrelation function of the residuals.[34,35]

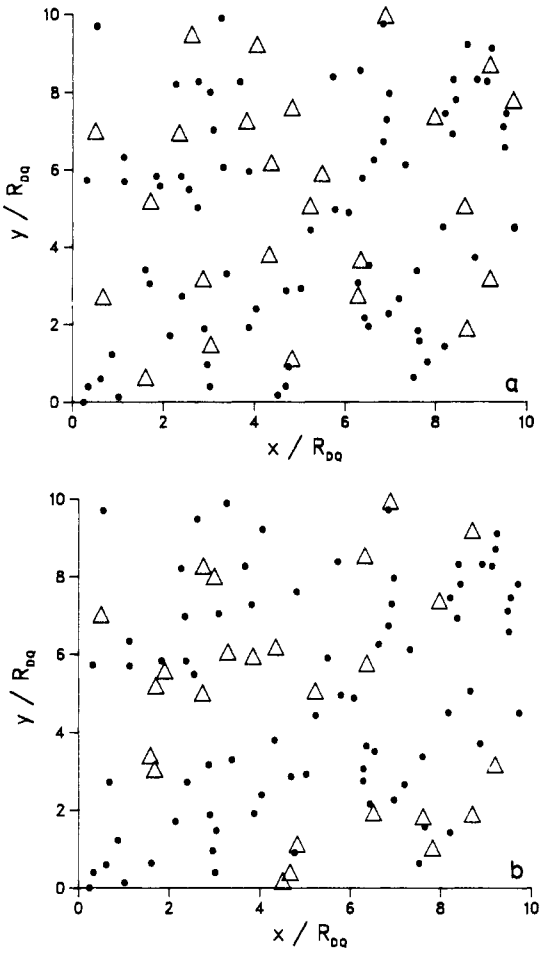

Figure 1. Comparison of random and nonrandom chromophore distributions in two dimensions. (a) Nonrandom distribution generated by Monte Carlo simulation of the gradual buildup of photoproducts that act as quenchers. In each distribution C_D = 0.589, C_Q = 0.785, and R_{DQ}/R_{DD} = 2.0. (b) Random distribution generated by arbitrarily relabeling donor chromophores (●) as quenchers (△) until a preset conversion has been reached.

Results and Discussion

Visualization of the Nonrandom Distribution. Figure 1 compares representative donor (●) and quencher (△) chromophore distributions that correspond to the random and nonrandom cases. The random distribution was generated by laying down a random initial distribution of donors in two dimensions and then arbitrarily selecting a certain fraction of them to be relabeled as quenchers.

The nonrandom distribution (Figure 1a) was generated from the same random donor distribution by the simulation in two dimensions of the gradual conversion to quenching photoproducts. In each case the degree of conversion was the same. In a representative random distribution (Figure 1b), there are a sizable number of quenchers that lie closer together than R_{DQ}. The energy-transfer behavior of this ensemble at very short times is dominated by fluorescence from donors quenched by photo-Fries products whose domains overlap in this way. In contrast the nonrandom distribution shows an absence of quenchers closer together than R_{DQ}. The effect on energy trapping is to increase the efficiency of quenching over the random chromophore distribution, but without producing short-time effects in the donor fluorescence decay characteristic of overlapping quenching domains. We have also attempted to illustrate the difference between these two distributions by calculating the average radial pair-distribution function $g(r)$ as a function of r/R_{DQ}. This function is shown in Figure 2a,b for nonrandom distributions and in Figure 2c for a random distribution. The minimum distance between quenchers has been set at $0.2R_{DQ}$ because of the excluded volume effect. Notice in Figure 2c the resemblance to the radial distribution function for a gas, while in Figure 2a,b there is a more structured behavior, somewhat reminiscent of the behavior in a crystalline solid.

In a preliminary study we have observed that a distribution characterized by a hard-sphere separation of R_{DQ} between quencher chromophores was a surprisingly accurate representation of the nonrandom distribution generated by the detailed Monte Carlo simulation. This hard-sphere model was not developed further, because we believe that its physical basis is less satisfactory than the model proposed here.

Tests of Simulation Performance. The simulations were modified to explore the effects of ensemble size and of the number of nearest donors and quenchers considered in calculation of the probabilities in eqs 6 and 7. To test the effects of ensemble size, a series of simulations was conducted at $C_D = 3.77$, $C_Q = 0.42$, and $R_{DQ} = R_{DD} = 1.0$ nm for different box sizes. This donor concentration is at least 7 times higher than that used in subsequent modeling of nonrandom chromophore distributions for comparison with experimental data. Both the high value of C_D and the low value of R_{DQ} were chosen to maximize the effects of energy migration within the donor ensemble. The time dependence of the ensemble-average donor excitation survival probability $G(t)$ was determined for various outer box sizes, while maintaining a constant inner box size of $(2R_{DQ})^3$ within which excitation of the donor chromophores occurred. For small ensemble sizes, boundary effects appeared to lower the efficiency of energy transport between donor chromophores (and hence the efficiency of energy trapping) so that $G(t)$ decayed too slowly with time. When ensemble sizes were increased eightfold or more, such edge effects appeared to vanish for this donor concentration, so that the behavior of $G(t)$ was essentially the same for cubes with sides of length $8R_{DQ}$ and $10R_{DQ}$. On the one hand, this study has established that a system with reduced concentration $C_D = 3.77$ is free of significant boundary effects, so that confidence can be placed in our Monte Carlo simulations, the bulk of which have been conducted at much lower reduced concentrations, typically $C_D = 0.25$. On the other hand, these results also suggest that Monte Carlo simulations of energy transfer, conducted on small ensembles[36] of chromophores for large C_D and small C_Q ($\gamma \rightarrow 100$, $\chi \rightarrow 1$ in ref 36) without periodic boundary conditions, might contain substantial edge effects.

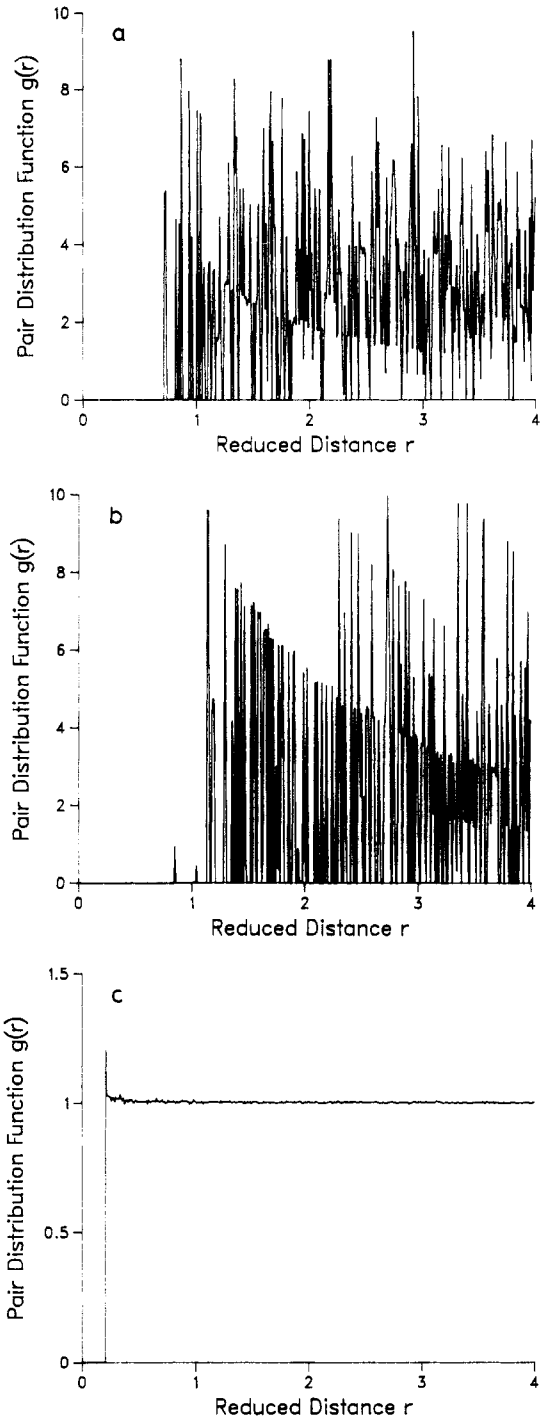

Figure 2. Comparison of the pair distribution functions between random distribution and nonrandom distributions for two dimensions: (a) nonrandom distribution, $y = 25\%$; (b) nonrandom distribution, $y = 15\%$; (c) random distribution, $y = 25\%$. The initial reduced donor concentration $(C_D)_0 = \pi/4$, with definition of $C_D = \pi R_{DD}^2 n_D$.[17]

The second model test was simply to identify the fastest way of performing the Monte Carlo simulation that did not result in distortion of information. The effect on the time dependence of $G(t)$ of truncation of the calculation of the transfer probabilities in eq 6 at the level of from 1 to 5 nearest-neighbor donors around the photoexcited chromophore showed that although consideration of only the nearest donor gives a representation of $G(t)$ that is anomalous, consideration of 2–5 donors already appears to result in limiting behavior for $G(t)$. A similar test was

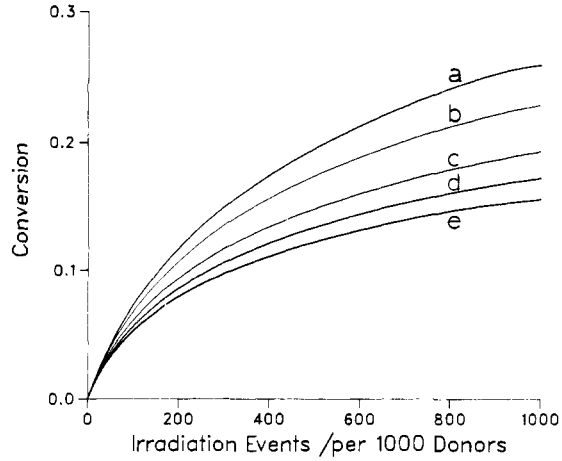

Figure 3. Variation of extent of conversion to photo-Fries products with number of excitation events, calculated by Monte Carlo simulation for different initial donor concentrations. In each case R_{DQ}/R_{DD} = 3.0, and the quantum yield of photoreaction is 0.1. Initial values of C_D are (a) 0.0888, (b) 0.134, (c) 0.268, (d) 0.524, and (e) 1.072.

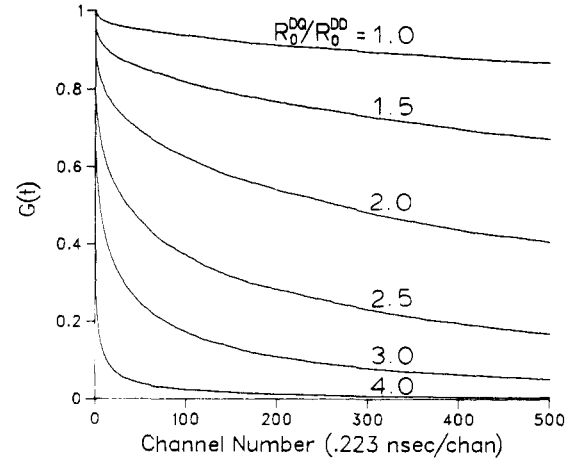

Figure 4. Variation of the donor decay profile function $G(t)$ with the ratio R_{DQ}/R_{DD} for nonrandom distributions at 10% conversion to photoproducts.

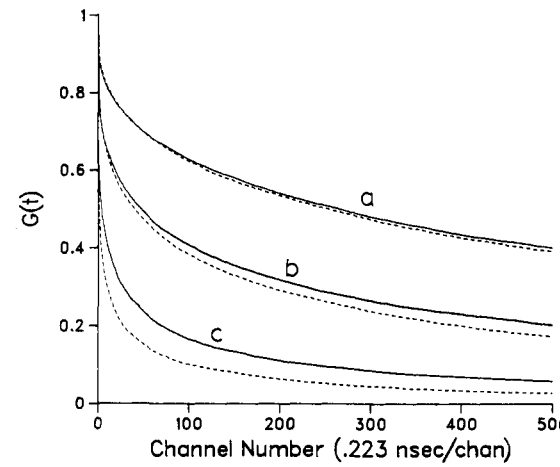

Figure 5. Comparison of donor decay profile functions $G(t)$ simulated for random (solid lines) and nonrandom (dashed lines) chromophore distributions. The initial reduced donor concentration C_D = 0.268 and R_{DQ}/R_{DD} = 2.5. Degrees of conversion are (a) 0.05, (b) 0.10, and (c) 0.20.

performed with truncation of the calculation of the transfer probability of eq 7 at 1–4 nearest quenchers around each photoexcited donor. The function $G(t)$ is even less sensitive to truncation of the number of quenchers than it is to truncation of the number of donors, because energy trapping is dominated by Förster transfer to the nearest quencher.

Characteristics of the Monte Carlo Model. Figure 3 shows the change in the extent of conversion to photoproducts, defined in eq 10, with the number of excitation events (proportional to irradiation time), calculated by Monte Carlo simulation for different initial chromophore concentrations. Strong inhibition of the reaction as a result of quenching by the photoproducts is observed, in agreement with experimental data for 2-naphthyl acetate dispersed in poly(methyl methacrylate) matrices.[30] The leveling off of the conversion–time graph occurs at decreasing conversion as the initial concentration of donors increases. This is because in the absence of energy migration the rate of conversion slows down once the quencher concentration reaches a reduced value of C_Q of around 1.0; this represents a different degree of conversion for each initial value of C_D. The effect of energy migration is to cause the conversion–time curves to level off at even lower values of C_Q.

It is no surprise that the function $G(t)$ generated for nonrandom chromophore distributions is sensitive to the relative magnitudes of the Förster radii R_{DD} and R_{DQ}. Certainly this is the case for random donor and quencher distributions.[13] Figure 4 illustrates the effect of changing the ratio R_{DQ}/R_{DD} on the function $G(t)$ for a fixed box size of side length $10R_{DQ}$. The large change in the rate of decay of $G(t)$ with changes in R_{DQ}/R_{DD} suggests that this ratio might serve as an adjustable parameter in comparing Monte Carlo and experimental results. We resisted this temptation because it was felt that, despite the difficulties of determining R_{DD} and R_{DQ} precisely, the value of the ratio should be independent of donor and acceptor chromophore concentrations and therefore independent of degree of conversion for all the experimental studies, so that it was inappropriate to make it an adjustable parameter.

If instead of varying R_{DQ}/R_{DD}, this ratio is held constant and C_Q is changed, then increased quenching by photo-Fries products with increasing conversion leads to more rapid decay in the function $G(t)$. This in turn causes further conversion to become progressively more difficult, behavior that can already be deduced from the conversion–time graphs of Figure 3.

It is interesting to compare Monte Carlo simulations of energy migration and transfer obtained for random and nonrandom chromophore distributions. In order to do this, random distributions of donors and quenchers in three dimensions were generated by first constructing random donor ensembles and then arbitrarily relabeling a portion of them as quenchers, following selection with a pseudo-random number generator. Energy transport and trapping within these ensembles were then modeled in exactly the same way as for the nonrandom distributions. Figure 5 compares the functions $G(t)$ obtained for the two types of distribution at the same overall degrees of conversion. In each case the function $G(t)$ decays more rapidly for the nonrandom chromophore distribution than for the corresponding random distribution. Moreover, the differences between the two curves increase with increasing conversion to photoproducts. This simulation is in agreement with an earlier qualitative prediction that the degree of nonrandomness in these donor/quencher systems should increase with increasing conversion.[30]

Before comparing this simulation with our experiments, we checked our statistics by computing a standard deviation for a typical $G(t)$ curve according to the method

Table I
Best-Fit Preexponential Factors A and Lifetimes τ (ns) of Experimental Fluorescence Decays for 0.115 M 2-Naphthyl Acetate in PMMA Immediately after 280–320-nm Irradiation[a]

irrad time, min	A_1; A_2; A_3	τ_1; τ_2; τ_3	$\langle\tau\rangle$[b]	χ_R^2
7	0.23;0.32;0.45	1.38;9.30;21.38	18.09	1.38
12	0.22;0.36;0.41	2.22;9.91;20.84	17.02	1.39
20	0.42;0.35;0.23	1.27;8.34;19.56	14.21	1.34
60	0.53;0.34;0.14	1.73;7.06;17.65	10.72	1.25

[a] Triple-exponential fitting function shown in eq 17. [b] Mean lifetime, defined in eq 18.

described in ref 37. The result shows that it was nowhere greater than 1.7%, and for more than half of the channels, it was less than 0.75%.

Comparison between Simulation and Experiment. The experimental fluorescence decays of 2-naphthyl acetate in poly(methyl methacrylate) films recorded at different degrees of conversion to photo-Fries products (eq 1) have features that make them clearly different from donor decays for randomly distributed chromophore systems.[30] Table I lists values of the lifetimes and preexponential factors for several such decays fitted to a three-exponential function (eq 17).

$$I_D(t) = A_1 \exp(-t/\tau_1) + A_2 \exp(-t/\tau_2) + A_3 \exp(-t/\tau_3) \quad (17)$$

This function merely represents a way of fitting the observed decays without reference to any energy-transfer mechanism.[38] For such a decay one can speak of a mean lifetime $\langle\tau\rangle$, defined in eq 18.

$$\langle\tau\rangle = \frac{A_1\tau_1^2 + A_2\tau_2^2 + A_3\tau_3^2}{A_1\tau_1 + A_2\tau_2 + A_3\tau_3} \quad (18)$$

Donor fluorescence decays recorded for nonrandom chromophore distributions had lower values of $\langle\tau\rangle$ than decays recorded for random distributions with the same donor and acceptor concentrations. At the same time, however, the decays for the nonrandom distributions are steeper at very short times than are the predictions of the Förster or Loring–Andersen–Fayer models, which are based upon random distributions.[30]

For comparison with these experimental fluorescence decay curves, simulations were conducted with R_{DQ}/R_{DD} fixed at 2.5, R_{DD} = 1.0 nm, and an initial reduced donor concentration C_D of 0.268, equal to the experimental donor concentration. Values of the degree of conversion y were adjusted to give the best fit between experimental and simulated fluorescence decays. In this sense the simulation contains a single adjustable parameter, although we note that y must at all times retain physically meaningful values. Thus y must increase with irradiation time and can at no time be greater than 0.25. A comparison has been carried out between the current Monte Carlo simulations for nonrandom distributions and experimental data obtained from films with both nonrandom and random donor/acceptor distributions having the same degrees of conversion.

Figures 6 and 7 compare experimental and simulated donor decay curves for two different degrees of conversion. The agreement between the experimental decays and the simulations based on nonrandom distributions is quite remarkable. Thus these two particular data sets gave reduced chi-squared values of χ_R^2 = 1.30 and 1.29, and there is no systematic deviation in the plots of the weighted residuals shown under each decay curve. The autocorrelation functions $C(j)$ of the weighted residuals are further evidence of good agreement between experimental and

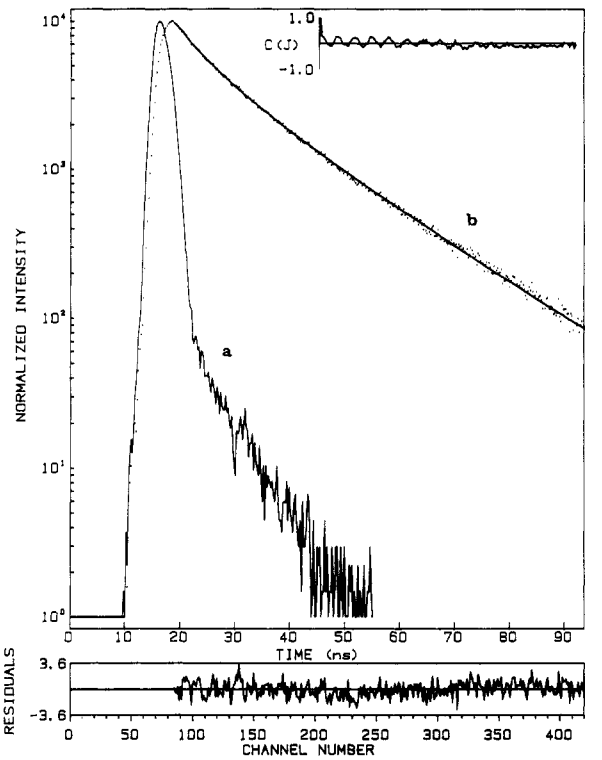

Figure 6. Comparison of experimental and simulated donor fluorescence decay curves. (a) Instrument response function. (b) Points: experimental fluorescence decay of 2-naphthyl acetate in poly(methyl methacrylate) film after 20 min of 280–320-nm irradiation to generate photo-Fries products in the matrix, excitation at 285 nm; solid line: best-fit donor fluorescence decay curve obtained by Monte Carlo simulation with nonrandom chromophore distributions. Under the decay curve is the channel-by-channel plot of the weighted residuals. The inset at the top right shows the autocorrelation function $C(j)$ of the residuals. The value of χ_R^2 for this analysis is 1.30.

simulated decay curves. The main source of deviation appears to be an experimental one, consisting of a small component of rf noise superimposed on the experimental decay curves. This gives rise to the low-frequency oscillations in the autocorrelation function. It is worth noting that it is not necessary to conduct Monte Carlo simulations to machine accuracy for comparison with single-photon-counting fluorescence decay data. The error properties of photon-counting data are well-known to obey Poisson statistics.[34] It has been shown in the literature that the superposition of random noise on an analytical trial function up to the limits allowed by Poisson statistics neither reduces nor enhances the quality of the fit to the experimental data.[39]

Table II lists values of the best-fit simulation parameters corresponding to a broad range of irradiation times. The agreement between experimental (nonrandom) and simulated donor fluorescence decay curves, summarized only by the χ_R^2 values, is good at all degrees of conversion (the fifth column of Table II). This is not only the case at short irradiation times, where the deviation of the donor decays from exponentiality is small, but also applies to higher degrees of conversion, where strongly nonexponential donor decays are observed. Furthermore, the values for the degrees of conversion to photoproducts generated by the best-fit simulations are all physically meaningful and correspond closely to the spectroscopically determined experimental values.

The same simulated donor fluorescence decay curves (based upon nonrandom chromophore distributions) were also compared with experimental decay curves associated

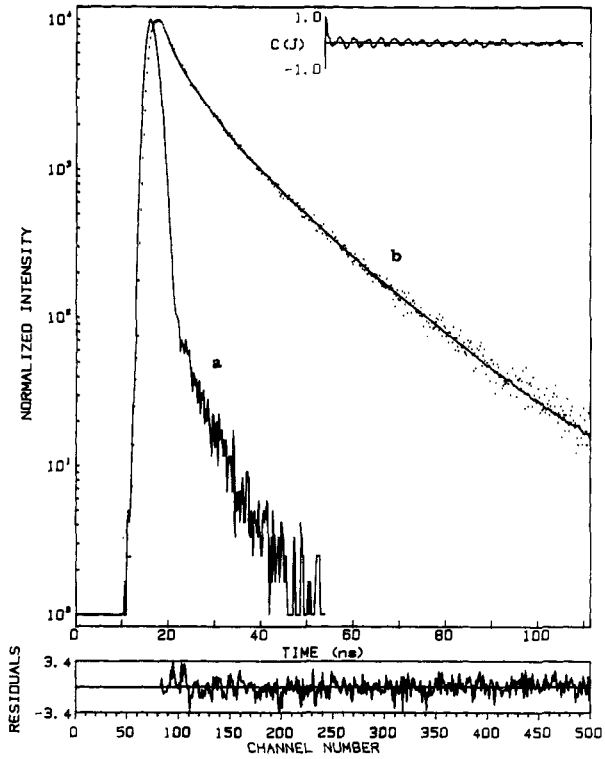

Figure 7. Comparison of experimental and simulated donor fluorescence decay curves. (a) Instrument response function. (b) Points: experimental decay for 2-naphthyl acetate in PMMA after 60 min of UV irradiation, λ_{ex} = 285 nm; solid line: best-fit decay obtained by Monte Carlo simulation with nonrandom chromophore distributions. For this analysis χ_R^2 = 1.29.

Table II
Comparison of Agreement between Donor Fluorescence Decays Calculated by Monte Carlo Simulations and Experimental Decays for 0.115 M 2-Naphthyl Acetate in PMMA

irrad time, min	conv	simulation C_D	simulation C_Q	χ_R^2 nonrandom distrib	χ_R^2 random distrib
4	0.048	0.255	0.201	1.66	16.2
7	0.079	0.247	0.331	1.79	21.9
12	0.100	0.241	0.418	1.48	32.3
20	0.148	0.228	0.620	1.30	84.0
>30	0.169	0.223	0.708	1.68	117.3
60	0.228	0.207	0.955	1.29	198.6

[a] Initial C_D = 0.268; R_{DQ}/R_{DD} = 2.5.

with random chromophore distributions (obtained by solvent treatment[30]): the results of this comparison are listed in the final column of Table II. The distinctly different χ_R^2 values found in the final two columns indicate that the fluorescence decay curves associated with nonrandom and random chromophore distributions can readily be distinguished. This view is corroborated by examination of Table III of ref 30, in which donor decay curves based upon the Förster and Loring–Andersen–Fayer models have also been compared with the experimental results obtained immediately after irradiation and after the film has been treated with toluene and then redried. The calculations based upon random chromophore distributions[30] gave good agreement with the experimental fluorescence decay curves obtained from the solvent-treated film and poor agreement with the decay curves obtained from the unmodified film. In both cases, the χ_R^2 deviations for the inappropriate chromophore distribution increase as the degree of conversion increases, while the corresponding χ_R^2 deviations for the appropriate chromophore distributions remain roughly unchanged.

Conclusions

Interest in the photophysics of nonrandom chromophore distributions would be slight if the deviation from random distributions were small. In the present situation we have demonstrated that the particular nonrandom distribution generated when a reactant is converted photochemically into a long-range quencher results in readily detectable changes in the photophysics of the system. Monte Carlo simulation has been a powerful tool both for visualizing this nonrandom distribution and for modeling the link between the chromophore distribution and its observable fluorescence behavior. Although an analytical representation of this particular nonrandom distribution is not available, a useful conceptual picture of the distribution is that it appears as though it contains a hard-sphere minimal repulsion distance of R_{DQ} between quenchers, but without corresponding restrictions on donor–donor and donor–quencher separations. Moreover, the Monte Carlo simulations have confirmed that donor fluorescence decays respond sensitively to deviations from random distributions. A similar conclusion has formed the basis for much of the recent work of Fayer, for example.[25,40]

It is worth noting the features of the model that were essential to achieve close agreement with experiment, as well as which refinements could be omitted. Essential features include an accurate representation of the nonrandom distribution, correct donor and quencher concentrations, and realistic values for R_{DQ} and R_{DD}. It has been found possible to perform the simulation with spherically averaged Förster transfer rates, without apparent loss of accuracy. This is in agreement with theoretical models of energy migration and transfer developed by Fayer and co-workers,[9,13] as well as with a Monte Carlo simulation by Riehl[17] which suggests that for randomly oriented chromophores the differences between spherically averaged and detailed orientation-dependent calculations are small. A second nonessential feature for successful agreement between Monte Carlo and experimental fluorescence decay data is continuation of the simulation until full machine accuracy is reached. It has been found to be necessary only to conduct the simulation until the noise level in the function $G(t)$ is small relative to the noise level in the experimental data. Indeed, it appears to us to be more useful to conduct less accurate simulations on large ensembles than it is to conduct machine-precision simulations on ensembles that are necessarily so restricted that artifacts of small ensemble size are introduced. Finally, a third nonessential feature for good agreement between experiment and simulation is the consideration of other types of interactions between chromophores, such as exchange or quadrupolar interactions. It is intriguing that energy transfer between naphthalene chromophores appears to be described adequately by the Förster mechanism, even though the Förster radius is quite small at only 1.0 nm.

There are many other types of nonrandom distributions in addition to that considered in this publication which can arise from polymer photochemistry. Examples include unusual spatial arrangements of chromophores arising from photo-cross-linking or from photoxidation occurring under conditions such as slow diffusion. It is expected that Monte Carlo simulation will be an indispensable tool for studying the effects of chromophore distribution in polymer photodegradation.

Acknowledgment. This research has been supported by grants in aid of research from the Natural Sciences and

Engineering Research Council of Canada. Z.W. thanks the University of Waterloo and the Ontario Ministry of Colleges and Universities for scholarship support. We are grateful to the reviewers for helpful comments on the original manuscript.

References and Notes

(1) Förster, Th. *Ann. Phys.* **1948**, *2*, 55.
(2) Förster, Th. *Z. Naturforsch. A* **1949**, *4*, 321.
(3) Galanin, M. D. *Sov. Phys.-JETP (Engl. Transl.)* **1955**, *1*, 317.
(4) Eisenthal, K. B.; Siegel, S. *J. Chem. Phys.* **1964**, *41*, 652.
(5) Leibowitz, M. *J. Phys. Chem.* **1965**, *69*, 1061.
(6) Dow, J. D. *Phys. Rev.* **1968**, *174*, 962.
(7) Burshtein, A. I. *Sov. Phys.-JETP (Engl. Transl.)* **1972**, *35*, 882.
(8) Haan, S. W.; Zwanzig, R. *J. Chem. Phys.* **1978**, *68*, 1879.
(9) Gochanour, C. R.; Andersen, H. C.; Fayer, M. D. *J. Chem. Phys.* **1979**, *70*, 4254.
(10) Blumen, A.; Manz, J. *J. Chem. Phys.* **1979**, *71*, 4694.
(11) Huber, D. L. *Phys. Rev. B* **1979**, *20*, 2307.
(12) Huber, D. L. *Phys. Rev. B* **1979**, *20*, 5333.
(13) Loring, R. F.; Andersen, H. C.; Fayer, M. D. *J. Chem. Phys.* **1982**, *76*, 2015.
(14) Beddard, G. S.; Porter, G. *Nature* **1976**, *260*, 366.
(15) Blumen, A.; Zumofen, G. *Chem. Phys. Lett.* **1980**, *70*, 387.
(16) Hilmes, G. L.; Harris, H. H.; Riehl, J. P. *J. Lumines.* **1983**, *28*, 135.
(17) Riehl, J. P. *J. Phys. Chem.* **1985**, *89*, 3203.
(18) Błoński, S.; Sienicki, K. *Macromolecules* **1986**, *19*, 2936.
(19) Knoester, J.; Van Himbergen, J. E. *J. Chem. Phys.* **1987**, *86*, 3577.
(20) Engström, S.; Lindberg, M.; Johansson, L. B.-A. *J. Chem. Phys.* **1988**, *89*, 204.
(21) Byers, J. D.; Friedrichs, M. S.; Friesner, R. A.; Webber, S. E. *Macromolecules* **1988**, *21*, 3402.
(22) Berberan-Santos, M.; Prieto, M. J. E. *J. Chem. Phys.* **1988**, *88*, 6341.
(23) Gösele, U.; Klein, U. K. A. *Acta Phys. Chem.* **1977**, *23*, 89.
(24) Ediger, M. D.; Fayer, M. D. *Macromolecules* **1983**, *16*, 1839.
(25) Zimmt, M. D.; Petersen, K. A.; Fayer, M. D. *Macromolecules* **1988**, *21*, 1145.
(26) Fredrickson, G. H.; Frank, C. W. *Macromolecules* **1983**, *16*, 572.
(27) Fredrickson, G. H.; Frank, C. W. *Macromolecules* **1983**, *16*, 1198.
(28) Fredrickson, G. H.; Andersen, H. C.; Frank, C. W. *Macromolecules* **1984**, *17*, 54.
(29) Boulu, L. G.; Patterson, L. K.; Chauvet, J. P.; Kozak, J. J. *J. Chem. Phys.* **1987**, *86*, 503.
(30) Wang, Z.; Holden, D. A.; McCourt, F. R. W. *Macromolecules* **1990**, *23*, 3773.
(31) Bellus, D. *Adv. Photochem.* **1971**, *8*, 109.
(32) Merle-Aubry, L.; Holden, D. A.; Merle, Y.; Guillet, J. E. *Macromolecules* **1980**, *13*, 1138.
(33) Holden, D. A.; Jordan, K.; Safarzadeh-Amiri, A. *Macromolecules* **1986**, *19*, 895.
(34) O'Connor, D. V.; Phillips, D. *Time-correlated Single Photon Counting*; Academic Press: London, 1984.
(35) Holden, D. A. In *CRC Handbook of Organic Photochemistry*; Scaiano, J. C., Ed.; CRC Press: Boca Raton, FL, 1989; Vol. 1, p 261.
(36) Błoński, S.; Bojarski, C. *Z. Naturforsch. A* **1989**, *44*, 257.
(37) Allen, M. P.; Tildesley, D. J. *Computer Simulation of Liquids*; Oxford University Press: Oxford, 1989; p 191.
(38) Meech, S. R.; O'Connor, D. V.; Roberts, A. J.; Phillips, D. *Photochem. Photobiol.* **1981**, *33*, 159.
(39) Nemzek, T. L. Ph.D. Thesis, University of Minnesota, 1975.
(40) Petersen, K. A.; Stein, A. D.; Fayer, M. D. *Macromolecules* **1990**, *23*, 111.